Diffraction and focusing of spectral energy in multiphoton processes

B. Broers and L. D. Noordam
FOM—Institute for Atomic and Molecular Physics, Kruislaan 407, 1098 SJ Amsterdam, The Netherlands

H. B. van Linden van den Heuvell
FOM—Institute for Atomic and Molecular Physics, Kruislaan 407, 1098 SJ Amsterdam, The Netherlands and Van der Waals–Zeeman Laboratorium, Valckenierstraat 65, 1018 XE Amsterdam, The Netherlands
(Received 13 March 1992)

We demonstrate an analogy between a two-photon process driven by a chirped pulse and Fresnel diffraction from a slit: in both situations interference between different "paths" leading to the same "final state" determines the resulting "diffraction pattern." On the basis of this analogy, a spectral Fresnel zone plate was designed for "focusing of spectral energy": at the two-photon level the spectral energy can be concentrated in an effective bandwidth that is much smaller than the bandwidth of the original excitation pulse. To show this effect, two experiments were performed with femtosecond laser pulses with a well-controlled power spectrum and chirp: frequency doubling in a nonlinear crystal and two-photon excitation of Rydberg states in rubidium.

PACS number(s): 42.65.−k, 42.79.Ci, 32.80.Rm

I. INTRODUCTION

In this paper we discuss an effect that could be called "spectral focusing in a multiphoton process." By this we mean that at a multiphoton level, the spectral energy can be concentrated in an effective bandwidth which is much smaller than the bandwidth of the original excitation pulse. This is schematically depicted in Fig. 1 for the case of a two-photon process driven by a pulse with central (angular) frequency ω_0 and bandwidth $\Delta\omega$. The expected "effective bandwidth" at the two-photon level, which slightly depends on the exact pulse shape, is approximately equal to $\Delta\omega$. We may now speak of spectral focusing at the two-photon level, if we can reach the situation in which the major part of the energy is concentrated in a bandwidth centered around $2\omega_0$, which is much smaller than $\Delta\omega$.

In our realization of this situation, the nonlinearity of a multiphoton process [1] plays a crucial role. In a one-photon process, a level at a certain energy above the initial state can only be excited by a photon of exactly that energy, irrespective of the bandwidth of the applied field. For a multiphoton process, however, this is no longer true. Due to the nonzero bandwidth of the excitation pulse, different combinations of photon energies add up to the same final energy, so that the final multiphoton excitation probability is determined by interference of the different excitation paths. Obviously, this interference is not necessarily constructive. The phase relations between the frequency components of the pulse, often called the "chirp" of the pulse, determine whether it is constructive or destructive. This is similar to the situation in which two light fields with different frequencies are applied to a system. If both fields can drive a certain transition, but with a different number of photons, then the total transition probability depends on the relative phase between the two fields (see, e.g., [2,3]).

In addition to the chirp, the power spectrum of the excitation pulse is important, since it determines the relative occurrence of the various frequencies, and hence the relative weight of the various excitation paths. This implies that the excitation probabilities at a multiphoton level critically depend on the amplitudes (power spectrum) and phases (chirp) of the frequency components of the pulse. An example of this subtle dependence was presented in Ref. [4], where the effect of a frequency chirp on the center of gravity of two-photon absorption peaks was considered.

For a two-photon process, the interference between the different excitation paths greatly resembles the interference between light paths after diffraction from a slit, resulting in a Frensel-diffracted pattern. This analogy will be discussed in greater detail in Sec. II. Thereafter, in Sec. III, several experimental results will be presented which illustrate this analogy. The experiments, frequency doubling in a nonlinear crystal and two-photon excitation of Rydberg states in rubidium, were performed with femtosecond laser pulses with well-defined power spectrum and chirp. Finally, in Sec. IV, it will be seen that this analogy can be used fruitfully; translating the ideas related to the well-known Fresnel zone plate to the situa-

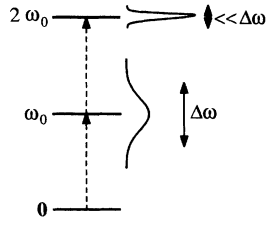

FIG. 1. The basic situation that could be termed spectral focusing, shown for a two-photon process. The effective bandwidth at the two-photon level is much smaller than the bandwidth $\Delta\omega$ of the excitation pulse.

tion of the two-photon process shows us how to choose the power spectrum and chirp to create pulses which indeed achieve spectral focusing at the two-photon level. Several experimental demonstrations of this effect will be given.

II. ANALOGY BETWEEN A TWO-PHOTON PROCESS AND FRESNEL DIFFRACTION

In this section we will discuss an analogy between a two-photon process driven by a chirped pulse and Fresnel diffraction from a slit. Consider a two-photon process driven by a pulsed field $E(t)$. The effective field that drives the two-photon process through the induced (nonlinear) polarization is then proportional to $E^2(t)$ (in the absence of intermediate resonances at the one-photon level). Its Fourier transform $E^{(2)}(\omega)$ determines the frequency response at the two-photon level. According to the well-known Fourier relationship between multiplication and convolution, $E^{(2)}(\omega)$ can be expressed as a (self-)convolution of $E(\omega)$, the frequency description of the original pulse:

$$E^{(2)}(\omega)=\int_{-\infty}^{\infty} d\omega' E(\omega')E(\omega-\omega') \ . \tag{1}$$

This formula expresses the notion that the effect of the pulse on one particular frequency at the two-photon level is found by a summation of all combinations of frequencies out of the fundamental pulse that add up to that particular frequency. Note that $E^{(2)}(\omega)$ peaks at $2\omega_0$, if $E(\omega)$ peaks at ω_0.

If we assume that $E(\omega)\equiv|E(\omega)|e^{i\phi(\omega)}$ is symmetric around ω_0, so $E(\omega_0+\delta\omega)=E(\omega_0-\delta\omega)$, then $E^{(2)}(\omega)$ at exactly twice the central frequency ω_0 reduces to

$$E^{(2)}(2\omega_0)=\int_{-\infty}^{\infty} d\omega'|E(\omega')|^2 e^{i2\phi(\omega')} \ . \tag{2}$$

So $E^{(2)}(2\omega_0)$ can be written as a simple sum over all frequencies of the fundamental pulse, each weighted by $|E(\omega)|^2$ (its power spectrum), taking into account the phase of each frequency component $\phi(\omega)$.

A similar type of sum over weighted phases is encountered when Fresnel diffraction from a slit is studied [Fig. 2(a)]. A line source L (directed perpendicular to the paper) illuminates a slit S (width Δz, extending from $z=-\frac{1}{2}\Delta z$ to $z=+\frac{1}{2}\Delta z$) at a distance L_1. The (Fresnel-) diffracted pattern is recorded on a screen P at a distance L_2 behind the slit. Calculating the diffracted intensity at P means summing up the contributions from all possible paths from L to P through a point z of the slit, taking into account the phase $\phi(z)$ of each contribution. The origin of the phase differences between the various paths is the difference in geometrical path lengths, relative to the wavelength of the light λ. For the point O, assuming $\Delta z \ll L_1, L_2$ this phase is given by

$$\phi(z)=\frac{\pi}{\lambda}\left[\frac{1}{L_1}+\frac{1}{L_2}\right]z^2 \tag{3}$$

(for a more rigorous treatment of Fresnel diffraction, see standard textbooks on optics, e.g., [5–7]). Note that $(1/L_1+1/L_2)$ is the sum of the curvatures of the wave fronts (=phase fronts) over the slit for waves coming from L and O, respectively.

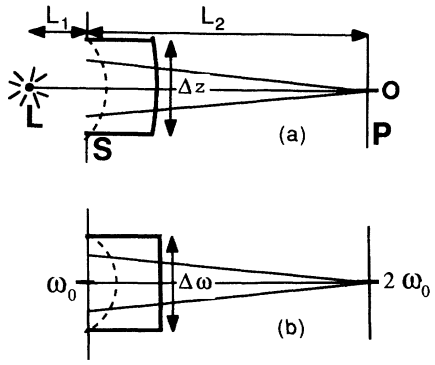

FIG. 2. The analogy between Fresnel diffraction from a slit and a two-photon process with a chirped pulse. (a) Fresnel diffraction: the line source L illuminates the slit S, and the diffraction pattern is recorded on the screen P. Each part of the slit contributes to the intensity at O with its own phase. Full and dashed curves represent the intensity and phase profile over the slit, respectively. (b) Two-photon process with a chirped pulse: each frequency within the fundamental bandwidth contributes to the intensity at $2\omega_0$ with its own phase. Full and dashed curves represent power spectrum and phase profile of the fundamental pulse, respectively.

If one now introduces a dimensionless form of z,

$$v=z\left[\frac{2}{\lambda}\left[\frac{1}{L_1}+\frac{1}{L_2}\right]\right]^{1/2} \ , \tag{4}$$

it is possible to write the diffractive field at O, E_O, in terms of the well-known Fresnel integrals (again, see [5–7]),

$$E_O \propto \int_{-\Delta v/2}^{+\Delta v/2} dv\, e^{i(\pi/2)v^2} \ . \tag{5}$$

Equation (5) indeed expresses the sum over phases $[\phi(v)=(\pi/2)v^2]$, similar to Eq. (2). It does not, however, contain a v-dependent weight factor. This is a result of the approximation $\Delta z \ll L_1, L_2$, which implies that the intensity over the slit is considered to be uniform. So in the case of both Fresnel diffraction and the two-photon process, a "path-integral" is encountered, summing up the various contributions of all paths and keeping track of the phase of each contribution.

These integrals, Eqs. (5) and (2), respectively, can then be mapped onto each other completely, if we drive the two-photon process with a pulse $E(\omega)=|E(\omega)|e^{i\phi(\omega)}$ with the following characteristics:

$$\begin{aligned} |E(\omega)| &= \begin{cases} E & \text{if } -\frac{1}{2}\Delta\omega \le (\omega-\omega_0) \le \frac{1}{2}\Delta\omega \\ 0 & \text{if } |\omega-\omega_0| > \frac{1}{2}\Delta\omega \ , \end{cases} \\ \phi(\omega) &= \alpha(\omega-\omega_0)^2 \ . \end{aligned} \tag{6}$$

The first requirement means that the power spectrum is square shaped with width $\Delta\omega$. This is the analog of the uniform illumination of the slits with width Δz. The second requirement means that the phase profile over the frequencies is quadratic, as is the phase profile over the slit. In $\phi(\omega)$, α measures the curvature of the phase

profile, as does $(1/\lambda)(1/L_1+1/L_2)$ in the case of Fresnel diffraction. This is schematically illustrated in Fig. 2(b). In the case of Fresnel diffraction, the diffraction pattern is fully determined by the dimensionless variable Δv, denoting the product of the slit width and the square root of the curvature of the phase front [see Eq. (4)]. One therefore expects the effect of the two-photon process to be fully determined by $\sqrt{\alpha}\Delta\omega$, which is also dimensionless. This is indeed the case, and we will come back to this point in Sec. III.

It should be noted that $E(\omega)$ as defined in Eq. (6) represents a chirped pulse since ϕ is not a linear function of ω [Fourier transformation of a pulse with a phase that depends on ω only linearly shows that such a phase causes a trivial translation of the pulse in time: $E(t)\rightarrow E(t+\tau)$; the pulse itself remains unchanged]. Due to this "quadratic phase chirp" the pulse has a time-dependent frequency. For example, Fourier transforming a pulse with a Gaussian envelope and a quadratic $\phi(\omega)$ results in $E(t)=|E(t)|e^{i(\omega_0+bt)t}=|E(t)|e^{i\phi(t)}$ (b is a constant), with $E(t)$ Gaussian and $\omega(t)\equiv\delta\phi(t)/\delta t$ changing linearly in time. Therefore such a chirp is often called a linear frequency chirp. However, for an arbitrary pulse shape, including the square-shaped $|E(\omega)|$ of Eq. (6), a phase of the form $\phi(\omega)=\alpha(\omega-\omega_0)^2$ does not imply that $\omega(t)$ is a linear function of time.

So far we have discussed the analogy for exactly twice the central frequency of the fundamental pulse $2\omega_0$ and the central part on the screen O. For frequencies detuned from $2\omega_0$ and points away from O, the analogy no longer strictly holds. The reason is that Fresnel diffraction represents a one-photon (linear) process, in contrast with the (nonlinear) two-photon process; in the case of Fresnel diffraction, every part of the slit contributes to the intensity at every part of the screen. On the other hand, not every frequency contributes to every frequency at the two-photon level because of energy conservation. For example, there is no frequency ω' within the bandwidth of the pulse such that $\omega'+(\omega_0-\frac{1}{2}\Delta\omega)=(2\omega_0+\frac{1}{2}\Delta\omega)$. Therefore the frequency $(\omega_0-\frac{1}{2}\Delta\omega)$ does not contribute to the frequency $(2\omega_0+\frac{1}{2}\Delta\omega)$ at the two-photon level. This exclusion mechanism would be the equivalent of a slit that is being closed as the diffraction pattern at a point away from O is recorded. The closing of the slit proceeds linearly with the distance from O; for observing the pattern at O the slit is opened completely, while for a distance Δz away from O, the slit is just closed. In mathematical form, this difference between the two-photon process and Fresnel diffraction can be seen from the integration boundaries when the generalized (detuned) forms of Eqs. (2) and (5) are considered:

$$E^{(2)}[2(\omega_0+\delta\omega)]\propto\int_{-\Delta\omega/2+|\delta\omega|}^{+\Delta\omega/2-|\delta\omega|}d\omega' e^{i2\alpha\omega'^2} \tag{7}$$

and

$$E_P(\delta v)\propto\int_{-\Delta v/2+|\delta v|}^{+\Delta v/2+|\delta v|}dv\, e^{i(\pi/2)v^2}, \tag{8}$$

where $E_P(\delta v)$ denotes the diffracted field at a point δv away from O. In the following discussion, we will not use this idea of the "variable slit width," since all important features of the analogy are already present in the case of a constant width.

III. EXPERIMENTAL DEMONSTRATION OF SPECTRAL DIFFRACTION

Since a Fresnel diffraction pattern shows diffraction fringes, one also expects, on the basis of the analogy described in the preceding section, "diffraction fringes" in two-photon excitation spectra resulting from pulses with a square-shaped power spectrum and a quadratic phase chirp. In this section, two experiments will be described in which these fringes are indeed observed: frequency doubling in a nonlinear crystal and two-photon excitation of Rydberg states in rubidium.

In order to perform these experiments with well-defined pulses, use was made of a laser system providing short pulses with accurately tunable wavelength, bandwidth, and chirp (for details, see [8]). Pulses from a colliding-pulse mode-locked (CPM) dye laser, with a central wavelength of 620 nm, were amplified in dye cells, which were pumped at 10 Hz by the second harmonic of a Nd:YAG (yttrium aluminum garnet) laser. To provide a tunable wavelength, these pulses were focused in water to generate a wavelength continuum. Selection of the desired wavelength was performed with a pulse shaper [9] (Fig. 3). This device consists of a grating, a lens, and a mirror placed in the focal plane of this lens, on which the various frequencies coming off the grating are separated. By placing a slit in front of the mirror, both central frequency and bandwidth of the pulse coming out of the shaper can be chosen arbitrarily. These pulses were amplified again to an energy of $\sim 20\ \mu$J. An example of a measured power spectrum of the amplified pulses is given as an inset in Fig. 3.

The shaper was also used to adjust the chirp of the pulses. If the distance between grating and lens is exactly the focal distance of the lens f, then the path length through the pulse shaper does not depend on the frequency. If, however, this distance is varied by Δx, different frequencies will no longer travel the same distance through the pulse shaper. This implies that the frequency spectrum of the pulse before the shaper, $E(\omega)$, is changed to $E(\omega)e^{i\phi(\omega)}$ after the shaper. If the bandwidth of the pulse is not too large (<10 nm), this extra phase is very well described by a Taylor expansion of ϕ, in which only the first nontrivial order is kept: $\phi(\omega)\approx\alpha(\omega-\omega_0)^2$, where α is proportional to Δx. The proportionality factor can be explicitly expressed in terms of experimental

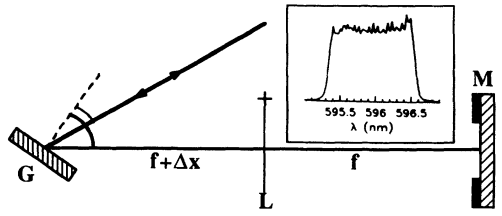

FIG. 3. Pulse shaper: G is the grating, L is the lens, and M is the mirror with a mask in front of it. Inset: square-shaped power spectrum of a pulse coming out of the shaper.

parameters: grating angles, grating spacing, and wavelength (see [10] for a more detailed description).

The first two-photon experiment we performed to demonstrate the diffraction fringes was optical second-harmonic generation (SHG) in a nonlinear crystal. With the pulse shaper, pulses were made with a central wavelength of 605.6 nm and a 2.8-nm bandwidth, corresponding to a chirp-free pulse duration of 380 fs. These pulses were frequency doubled in a KDP (potassium dihydrogen phosphate) crystal. The power spectrum of the frequency-doubled light was then measured with a monochromator (SPEX 1870) and an optical multichannel analyzer (EG&G 1453A). The length l of the KDP crystal was 0.5 mm, short enough to ensure that all frequencies within the bandwidth of the pulse were properly phase matched ($\Delta k_{\max} l = 0.4\pi$, where $\Delta k_{\max}$ is the maximal phase mismatch).

For three different values of the chirp α, the measured power spectra are given in Fig. 4(a). The spectra clearly shows wiggles: the diffraction fringes. The measured results are in very good agreement with the results of a calculation of $|E^{(2)}(\omega)|^2$, according to Eq. (1), using the pulse defined by Eq. (6).

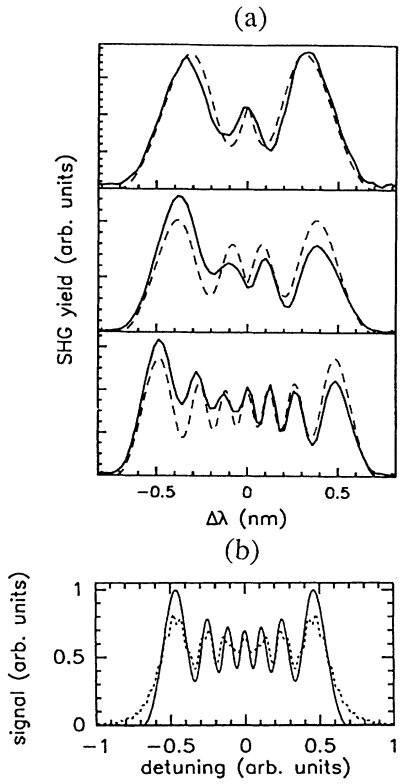

FIG. 4. (a) Experimental (full lines) and theoretical (dashed lines) power spectra of frequency-doubled light resulting from pulses with a square-shaped power spectrum and increasing values of the chirp. The wiggles can be seen as diffraction fringes at the two-photon level, resulting from interference between the various excitation paths. (b) Comparison between the shapes of the two-photon power spectrum resulting from the pulse with the largest chirp (full line) and the Fresnel diffracted pattern that results from the situation with a corresponding curvature of the phase front (dotted line) The label "detuning" refers to the frequency difference with the central frequency in the case of the two-photon process, and to the distance between a point and the central point on the screen in the case of Fresnel diffraction [see also Figs. 2(a) and 2(b)].

Despite the fact that the analogy is not perfect for frequencies detuned from $2\omega_0$, as pointed out in Sec. II, the properties of the fringes completely match those of Fresnel diffraction [Fig. 4(b)]: going from the center to either side of the pattern, the fringes become wider, the maximum of each fringe grows higher, and its minimum deepens (for a whole series of plots of Fresnel-diffraction patterns see, e.g., [7]).

To obtain some insight into the number of fringes, consider all combinations (ω_1,ω_2) that add up to $2\omega_0$: $\omega_1+\omega_2=2\omega_0$. It is clear that they have the form $\omega_1=\omega_0-\delta\omega$, $\omega_2=\omega_0+\delta\omega$ (where $-\frac{1}{2}\Delta\omega \le \delta\omega \le \frac{1}{2}\Delta\omega$). According to Eq. (6) this corresponds to phases $\phi_1=\phi_2=\alpha(\delta\omega)^2$, so that the total phase of such a path is $\phi_{\text{tot}}=\phi_1+\phi_2=2\alpha(\delta\omega)^2$. The largest phase difference occurs between the extreme paths—the one with $\delta\omega=0$ (so $\omega_1=\omega_2=\omega_0$) and the one with $\delta\omega=\frac{1}{2}\Delta\omega$ (so $\omega_1=\omega_0-\frac{1}{2}\Delta\omega$, $\omega_2=\omega_0+\frac{1}{2}\Delta\omega$)—$\Delta\phi_{\max}=\frac{1}{2}\alpha(\Delta\omega)^2$. If $\Delta\phi_{\max}$ amounts to $\approx\pi$ these extreme paths interfere destructively, which causes the development of a local minimum in the two-photon spectrum at $2\omega_0$. Equivalently, if $\Delta\phi_{\max}\approx 2\pi$ then the interference is constructive, resulting in a local maximum. Then, however, there will be two frequencies, detuned from $2\omega_0$, for which the extreme paths leading to these frequencies have a phase difference of π. This results in two local minima at these freuqencies, and so forth. This line of reasoning shows that the total number of peaks in the two-photon spectrum N can be estimated by

$$N \approx 1+\frac{\Delta\phi_{\max}}{\pi}=1+\frac{\alpha(\Delta\omega)^2}{2\pi}\ . \tag{9}$$

It is clear that N is completely determined by the dimensionless variable $\sqrt{\alpha}\Delta\omega$, which has already been mentioned in Sec. II. This can now be understood, because its square $\alpha(\Delta\omega)^2$ is a direct measure for the maximum phase difference over the excitation pulse. The values of $\alpha(\Delta\omega)^2$ for the results in Fig. 4 are 4.7π, 7.0π, and 13.6π, respectively. Consequently, on the basis of Eq. (9), one expects three, four, and seven fringes in the spectra, in accordance with the results.

In order to demonstrate that the observed diffraction fringes are a property of the two-photon process and not due to some spurious effects in the KDP crystal (e.g., phase-match conditions, depletion of the fundamental pulse), we also performed another experiment: two-photon excitation of electronic Rydberg states in rubidium, resulting almost exclusively in population of d states. The bandwidth of the excitation pulse (1.56 nm, corresponding to a chirp-free pulse duration of 680 fs) was large compared to the spacing of the levels, so that several states were excited around $nl=28d$. After excitation, the populations of the levels were probed with pulsed field ionization. The field-ionized electrons were detected with a channel plate. The electric-field strength of the ionizing pulse increased in time, so that the elec-

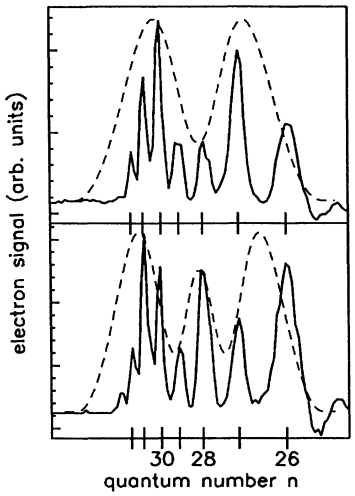

FIG. 5. Distributions of populations over Rydberg levels after two-photon excitation with pulses with a square-shaped power spectrum for two different values of the chirp. The dashed curves give the theoretically expected envelopes of the excitation spectra.

tron signal, recorded as a function of time, showed consecutive peaks corresponding to Rydberg levels with decreasing principal quantum number (for details, see [10]).

Two measured results, for $\alpha(\Delta\omega)^2=3.6\pi$ and 5.6π, are shown in Fig. 5, as well as the corresponding calculated envelopes for the distributions over the excited levels. The diffraction fringes are clearly visible in the envelopes. The main part of the discrepancy between the measured and calculated results can be attributed to the fact that the horizontal axis for the measured results represents a linear time scale which is not a linear energy scale, due to the characteristics of the field-ionizing pulse.

IV. EXPERIMENTAL DEMONSTRATION OF SPECRAL FOCUSING

One of the useful aspects of an analogy between two fields is the fact that it can often be used fruitfully to translate an idea well known in one field to another field where it has not yet been recognized. In this section, a translation will be given of the Fresnel zone plate, resulting in the possibility of spectral focusing in multiphoton excitation. Several experiments illustrating this effect will be discussed.

Although the principle of the Fresnel zone plate is discussed in many textbooks (e.g., [5]), we will briefly summarize the relevant ideas as a starting point of the subsequent extension. From Fig. 2(a) it is clear that the shortest path from the light source L to the central point on the screen O is the straight line LO. All other paths through the slit are longer, resulting in a phase difference between these paths and the direct one. For some paths this phase difference is $\approx 2\pi n$, resulting in constructive interference, while for others it is $\approx 2\pi(n+1)$, resulting in destructive interference. A mask in the slit which blocks those zones through which paths go that interfere destructively greatly enhances the intensity at O: the light is focused. Such a mask is called a Fresnel zone plate.

In practical situations, a Fresnel zone plate is used for focusing, instead of a normal lens, if no transparent lens material is available for the wavelengths of the light (or particles) that are to be focused. They have, for example, been used for the focusing of x rays [11], slow neutron beams [12] and, very recently, even atoms [13].

Returning to the analogy, one sees that it should be possible to enhance the spectral energy at $2\omega_0$ by blocking those paths to $2\omega_0$ that interfere destructively because of their phase difference with the shortest path. As was shown in Sec. II, the total phase of the path $(\omega_0-\delta\omega,\omega_0+\delta\omega)$, leading to $2\omega_0$, is given by $\phi_{\rm tot}(\delta\omega)=2\alpha(\delta\omega)^2$. One now has to divide the paths into zones, such that the maximum phase difference within one zone is π. The zone boundaries are given by $\delta\omega_n$, $n=1,2,\ldots,n_{\rm max}$, where $(n-1)\pi<\phi_{\rm tot}<n\pi$ for all values of $\delta\omega$ in the interval $(\delta\omega_{n-1},\delta\omega_n)$. The maximal phase $\phi_{\rm max}=\frac{1}{2}\alpha(\Delta\omega)^2$ determines $n_{\rm max}$. This is illustrated in Fig. 6 for the case of $n_{\rm max}=4$. Note that the width of the zones is not equal, since $\phi_{\rm tot}$ is not a linear function of $\delta\omega$. The width of the nth zone is proportional to $(\sqrt{n}-\sqrt{n-1})$, which approximately decreases with n like $1/\sqrt{n}$. The enhancement of energy at $2\omega_0$ can now be obtained by either blocking all odd frequency zones (n odd), or all even frequency zones (n even). This blocking removes the destructive interference between paths from neighboring zones which have a phase different of π.

Following the procedures of pulse shaping by Weiner, Heritage, and Kirschner [9], the obvious place to select the desired frequency intervals is right in front of the mirror in the pulse shaper (Fig. 3), since the frequencies are separated there. It would therefore suffice to put a mask in front of the mirror with open slits at those positions that correspond to, for example, all odd zones. However, there is an experimental problem: the frequencies on the mirrors are only focused down to the diffraction limit $d_{\rm lim}$, which is proportional to $\lambda f/D$, where f is the focal length of the lens, and D the diameter of the light beam before the shaper. Since it is useless to make slits with a width smaller than a few times the diffraction limit (such a slit cannot perform proper frequency selection), the number of Fresnel zones that can be used is limited. In order to make $d_{\rm lim}$ as small as possible, one can decrease f, or increase D. The first option, however, does not work, because the separation of the

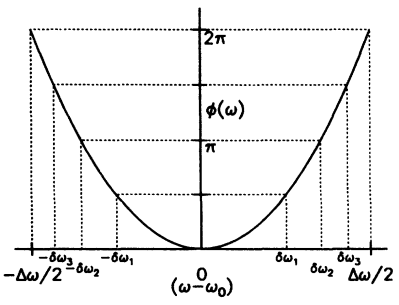

FIG. 6. The phase profile over the bandwidth divided into (Fresnel) zones: a new zone starts each time the total phase of a path to $2\omega_0$, $2\phi(\omega)$, exceeds an integer number of π.

frequencies on the mirror is also proportional to f. This implies that the "resolving power" of the shaper, which is the frequency separation divided by the diffraction limit, is independent of f. Consequently, D must be made as large as possible in order to decrease d_{lim}. In our case the practical limit of the beam diameter was $D \approx 13$ mm. In combination with $f = 250$ mm, this results in $d_{\text{lim}} \approx 30$ μm. This implies that the smallest useful slit width was ≈ 100 μm, which limited the number of zones to 6.

The actual total width of the zone plate we used was 2.0 mm, and contained a smallest zone of 97 μm. It was designed to pass the first three odd zones of an appropriately chirped pulse, and block the even ones. Note that the chirp α has to be adjusted to make the slits coincide with the actual Fresnel zones. The effect of the zone plate on the power spectrum of the pulse coming from the shaper can be seen in Fig. 7. All frequency intervals are well resolved.

The effect of the zone plate on freuqency doubling is shown in Fig. 8. In the left column measured power spectra of frequency-doubled light are given for four situations. The two results in the lower part of the figure were obtained with pulses having the same chirp, but a different form of the power spectrum. The dotted line represents the results for a pulse with a square-shaped power spectrum, a bandwidth of 1.6 nm and a chirp such that $\frac{1}{2}\alpha(\Delta\omega)^2 = 6\pi$, which amounts to six Fresnel zones. If the zone plate is used to block the even zones, the full line is meaured, clearly showing the enhancement of energy at $2\omega_0$ at the cost of energy at detuned frequencies.

The spectra of the frequency-doubled light given in the upper part of Fig. 8 werre obtained with chirp-free pulses having the same height of the power spectrum $I(\omega) = |E(\omega)|^2$ as the chirped pulses. The results show that one really can speak of focusing. The full curve results from a pulse with a bandwidth of 0.58 nm, which is equal to the width of the first (central) zone of the pulse described above. Although this pulse is chirp-free, the yield at $2\omega_0$ is lower than that of the focused result. Furthermore, the two-photon spectrum is a factor of 2.1 broader [full width at half maximum (FWHM)], while the bandwidth of this pulse is a factor of 2.5 *smaller* than that of the one used to obtain the focused result. If a chirp-free pulse is used with a bandwidth such that the frequency-doubled spectrum has the same width (FWHM) as the focused one, the dashed curve results. In this case, however, the yield at $2\omega_0$ is a factor of 6.7

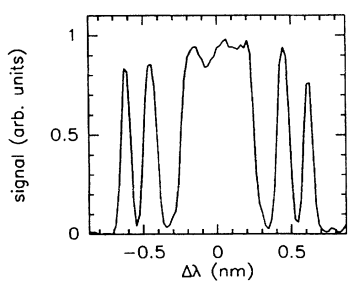

FIG. 7. Power spectrum of the excitation pulse, with the Fresnel zone plate put into the shaper. The zone plate blocks the first three even Fresnel zones.

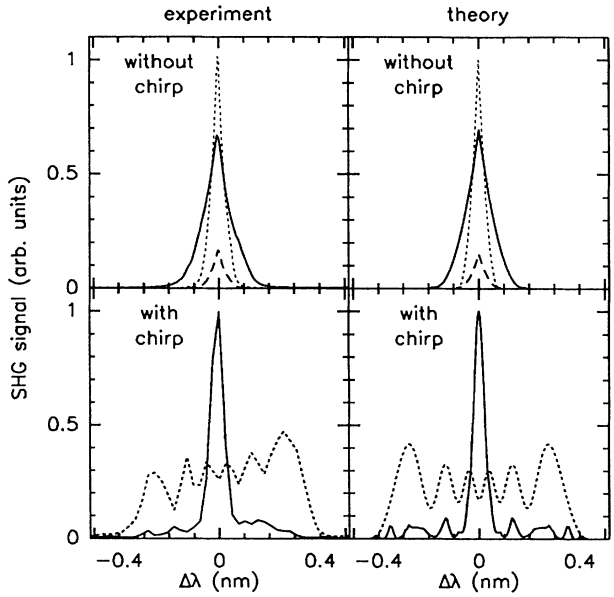

FIG. 8. Experimental (left) and theoretical (right) power spectra of frequency-doubled light for four situations, which show the effect of spectral focusing. Lower part: the dotted line results from a pulse with a chirp that amounts to six Fresnel zones. When the even Fresnel zones are blocked, the yield at $2\omega_0$ is enhanced at the cost of yield at detuned frequencies (full line). Upper part: results from chirp-free pulses. In the case of the full line, the bandwidth equals that of the first (central) Fresnel zone of the pulse used in the focused result. In the case of the dashed line the bandwidth is such that the width (FWHM) of the resulting frequency-doubled spectrum is the same as for the focused result. A (vertical) blowup by a factor of 6.7 is given for the dashed result (dotted line).

lower. The dotted curve is a 6.7× vertical blowup of the dashed one, drawn to facilitate comparison of the results. All measured results are reproduced well by calculations using Eq. (1) (right column of Fig. 8).

From the data in Fig. 8 it is clear that a chirp-free pulse cannot give the same combination of small spectral width and high yield at $2\omega_0$ as obtained by spectral focusing. Thus spectral focussing can be used for efficient selective excitation of one (discrete) level out of a series. For the case of two-photon excitation of Rydberg states in rubidium (see Sec. III), the basics of this notion are illustrated in Fig. 9. The dotted curve is the distribution of Rydberg levels resulting from the same chirped pulse as the one used to obtain the results of Fig. 8. Using the zone plate results in the distribution given by the full line, which mainly consists of one, efficiently excited, level.

As a more pronounced demonstration of the unique combination of high yield and good spectral resolution, a wavelength scan over the Rydberg series was made. The wavelength was scanned by rotating the grating of the pulse shaper with the help of a stepper motor. After the light pulse, the total population in the excited states, integrated over all levels, was measured. This was done by recording the total electron yield after pulsed field ionization. Figure 10(a) shows the result of the scan made with the focused light. It is seen that the levels $n \leq 28$ are

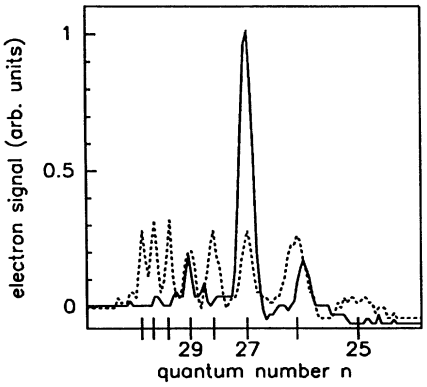

FIG. 9. The effect of spectral focusing shown in the case of two-photon excitation of Rydberg levels in rubidium: the dashed distribution results from a pulse with a chirp that amounts to six Fresnel zones. When the even Fresnel zones are blocked, the full line results, showing mainly one efficiently excited level.

completely resolved, while levels up to $n \approx 37$ can be identified.

If the scan is made with a chirp-free pulse having the same bandwidth as the first (central) zone of the chirped pulse used in the focused result, keeping $I(\omega)$ constant [Fig. 10(b)], the yield decreases slightly, as can be concluded from the vertical scale. The resolution, however, deteriorates much more drastically (compare with the full curve in the upper part of Fig. 8): now only levels $n \leq 24$ are fully resolved, while identification of the levels already stops at $n \approx 29$.

By reducing the bandwidth of the chirp-free pulse, one can, of course, reach a spectral resolution comparable to the case of the focused result. But then the yield decreases heavily [see Fig. 10(c) and compare with the dashed curve in the upper part of Fig. 8]. One may wonder why the signal-to-noise ratio seems the same in Figs. 10(a) and 10(c). The reason is that this ratio is infinitely good for both measurements; the shape of the "wiggles" at the short-wavelength side, where many Rydberg levels are excited by the same pulse, critically depends on the exact shape of the pulse, which is different for Figs. 10(a) and 10(c). The wiggles are real and not noise in the data. These results, once more, illustrate that a chirp-free pulse cannot reproduce the characteristics of the focused one, given a certain height of the power spectrum.

Instead of keeping the height of the power spectrum constant, one can also compare the effects of the focused pulse and the small-bandwidth pulse when they have the same average intensity $\bar{I}$ (which we define as the intensity averaged over the pulse area between the two points at half maximum). To do so, the height of the power spectrum of the small bandwidth pulse must be increased by a factor of 2.1. Consequently, its yield increases by a factor $(2.1)^2 = 4.4$, which means that it is still less than the yield of the focused result. Exactly the same numbers are found when the comparison is made for pulses with the same average of the intensity squared $\overline{I^2}$.

The width of the focused two-photon spectrum can be

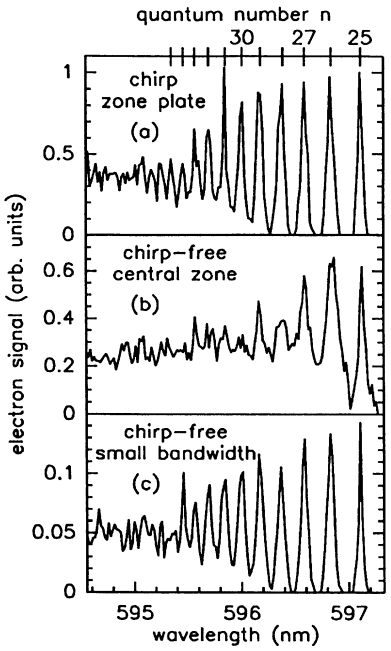

FIG. 10. Wavelength scan over Rydberg series in rubidium, showing the combination of both high yield and good resolution, resulting from spectral focusing. (a) shows the focused result: the chirp amounts to six Fresnel zones, and the (three) odd ones are passed through the zone plate in the pulse shaper. (b) Results from a chirp-free pulse with a bandwith equal to the wdith of the first (central) zone of the pulse used to obtain the focused result. The resolution deteriorates heavily compared to the focused result. In (c) the resolution has been improved again to the level of the focused result by reducing the bandwidth of the chirp-free pulse, keeping $I(\omega)$ constant, but this also reduces the yield (note the difference in vertical scales).

related to the chirp α and the bandwidth $\Delta\omega$. To do so, the equivalents of the chirp and the bandwith in terms of the corresponding parameters of Fresnel diffraction are useful (see Sec. II): $\alpha \leftrightarrow (1/\lambda)(1/L_1 + 1/L_2)$ and $\Delta\omega \leftrightarrow \Delta z$. Now suppose that the (normal) zone plate is used as a lens for a parallel beam with diameter D. This implies [see Fig. 2(a)] $\Delta z \rightarrow D$, $L_1 \rightarrow \infty$, and $L_2 = f$, where f denotes the focal length of the lens. Then the above-mentioned translations reduce to $\alpha \leftrightarrow 1/\lambda f$ and $\Delta\omega \leftrightarrow D$. Using these identifications the diffraction-limited width of a lens, which is proportional to $\lambda f/D$, translates to a diffraction limited width of the focused two-photon power spectrum which is proportional to $1/\alpha\Delta\omega$. Since the number of Fresnel zones N_z is proportional to $\alpha(\Delta\omega)^2$, the focal width is proportional to $\Delta\omega/N_z$ as well. This relationship was also verified with a computer program that calculated the effect of various spectral zone plates. It shows that the focusing power, given a certain bandwidth $\Delta\omega$, can largely be enhanced by increasing the number of Fresnel zones.

V. CONCLUSIONS

In this paper we have demonstrated an analogy between a two-photon process and Fresnel diffraction from

a slit. Although the latter process is linear (one photon), whereas the first is nonlinear, both a Fresnel-diffracted pattern and a two-photon power spectrum can be considered to result from interference between different paths leading to one final state. In the case of a multiphoton process, the different paths are formed by different combinations of frequencies out of the broad bandwidth of the pulse which add up to the same final energy. Since the phases of the frequencies are determined by the chirp of the excitation pulse, one can control the multiphoton excitation spectra by controlling chirp and bandwidth of the pulse.

Using these ideas, it is possible to shape pulses which give rise to focusing of spectral energy at the two-photon level: most of the energy at this level is then concentrated in an effective bandwidth which is much smaller than the bandwidth of the original excitation pulse. The characteristic power spectrum and chirp of these pulses result from the use of a spectral Fresnel zone plate, which is a translation of the conventional Fresnel zone plate. In several experiments it was demonstrated that the effect of spectral focusing offers a unique combination of high excitation yield and small effective bandwidth that cannot be obtained using chirp-free pulses, given a fixed height of the power spectrum of the pulses.

ACKNOWLEDGMENTS

The authors would like to express their sincere thanks to the infrared group at the FOM Institute for the loan of essential equipment, and to M. P. de Boer for critically reading the manuscript. The work described in this paper is part of the research program of the Stichting voor Fundamenteel Onderzoek van de Materie (Foundation for Fundamental Research on Matter) and was made possible by financial support from the Nederlandse Organisatie voor Wetenschappelijk Onderzoek (Netherlands Organization for the Advancement of Research).

[1] See, e.g., *Multiphoton Processes, Proceedings of the Fifth International Conference on Multiphoton Processes, Paris, 1990,* edited by G. Mainfray and P. Agostini (Service de Documentation du CEN, Saclay, 1991).

[2] H. G. Muller, P. H. Bucksbaum, D. W. Schumacher, and A. Zavriyev, J. Phys. B **23**, 2761 (1990).

[3] Ce Chen, Yi-Yian Yin, and D. S. Elliot, Phys. Rev. Lett. **64**, 507 (1990).

[4] M. S. Fee, K. Danzmann, and S. Chu, Phys. Rev. A **45**, 4911 (1992).

[5] E. Hecht, *Optics,* 2nd ed. (Addison-Wesley, Reading, MA, 1989), pp. 434–458.

[6] M. Born and E. Wolf, *Principles of Optics,* 1st ed. (Pergamon, London, 1959), pp. 427–434.

[7] F. A. Jenkins and H. E. White, *Fundamentals of Optics,* 3rd ed. (McGraw-Hill, New York, 1957), pp. 353–381.

[8] L. D. Noordam, W. Joosen, B. Broers, A. ten Wolde, A. Lagendijk, H. B. van Linden van den Heuvell, and H. G. Muller, Opt. Commun. **85**, 331 (1991).

[9] A. M. Weiner, J. P. Heritage, and E. M. Kirschner, J. Opt. Soc. Am. B **5**, 1563 (1988).

[10] B. Broers, H. B. van Linden van den Heuvell, and L. D. Noordam, Opt. Commun. **91**, 57 (1992).

[11] See, for example, *X-ray Microscopy,* edited by G. Schmahl and D. Rudolph, Springer Series in Optical Sciences Vol. 43 (Springer, Berlin, 1984).

[12] P. D. Kearney, A. G. Klein, G. I. Opat, and R. Gähler, Nature (London) **287**, 313 (1980).

[13] O. Carnal, M. Sigel, T. Sleator, H. Takuma, and J. Mlynek, Phys. Rev. Lett. **67**, 3231 (1991).